



Contents lists available at ScienceDirect

Bioorganic & Medicinal Chemistry Letters

journal homepage: www.elsevier.com/locate/bmcl

Syntheses of aminoalcohol-derived macrocycles leading to a small-molecule binder to and inhibitor of Sonic Hedgehog

Lee F. Peng^{a,b,c,*,†}, Benjamin Z. Stanton^{b,c,†}, Nicole Maloof^{b,c}, Xiang Wang^{b,c}, Stuart L. Schreiber^{b,c,d,‡}^a GI Unit, Department of Medicine, Massachusetts General Hospital, 55 Fruit Street, Boston MA 02114, United States^b Department of Chemistry and Chemical Biology, Harvard University, 12 Oxford St., Cambridge, MA 02138, United States^c The Broad Institute, 7 Cambridge Center, Cambridge, MA 02142, United States^d Howard Hughes Medical Institute, Broad Institute of Harvard and MIT, 7 Cambridge Center, Cambridge, MA 02142, United States

ARTICLE INFO

Article history:

Received 28 August 2009

Revised 18 September 2009

Accepted 22 September 2009

Available online 25 September 2009

This article is dedicated to the memory of
Brian L. Gray

Keywords:

Sonic Hedgehog

Robotnikinin

Macrocyclic

Small-molecule microarray

Surface plasmon resonance

Shh-LIGHT2

Ptc1^{-/-}

ABSTRACT

We report the synthesis and biological activity of a library of aminoalcohol-derived macrocycles from which robotnikinin (**17**), a binder to and inhibitor of Sonic Hedgehog, was derived. Using an asymmetric alkylation to set a key stereocenter and an RCM reaction to close the macrocycle, we were able to synthesize compounds for testing. High-throughput screening via small-molecule microarray (SMM) technology led to the discovery of a compound capable of binding ShhN. Follow-up chemistry led to a library of macrocycles with enhanced biological activity relative to the original hit compounds. Differences in ring size and stereochemistry, leading to alterations in the mode of binding, may account for differences in the degree of biological activity. These compounds are the first ones reported that inhibit Shh signaling at the ShhN level.

© 2009 Elsevier Ltd. All rights reserved.

Polyketide synthase-derived macrolactones are rich in structural diversity and biological activity. Examples include pikromycin¹ and erythromycin² (inhibitors of bacterial protein synthesis), enterobactin (inhibitor of bacterial iron transport),³ epothilones A, B, D (stabilizer of microtubules),⁴ and FK506 (inhibitor of PP2B phosphatase via its FKBP12 complex).^{5–7} We report here a synthesis of macrolactones that has yielded a powerful new small-molecule probe of the Hedgehog signaling pathway, which plays key roles in development and oncogenesis.

Our synthesis exploits 1,2-aminoalcohols as simple templates upon which 12-, 13- and 14-membered macrocycles are built (Scheme 1). The pathway extends previous work, reported by Lee et al., which also derived macrocyclic scaffolds from aminoalcohol templates, and yields macrocycles that can be optimized with great facility when they are identified as hits in small-molecule screens.⁸

We report herein a new asymmetric alkylation sequence to the pathway, a modification that installs a stereogenic center bearing an amide side-chain on the macrocycle scaffold and that resulted in a new scientific discovery. Starting from commercially available γ -unsaturated pentenoyl chloride, the Evans oxazolidinone,⁹ and readily available chiral 1,2-aminoalcohols, the target macrolactones were synthesized in nine steps. Following an asymmetric alkylation with α -bromo-*tert*-butyl acetate, which proceeded with over 19:1 diastereoselectivity, the *tert*-butyl ester was cleaved with TFA. The resulting acid was submitted to standard amine coupling conditions in the presence of a variety of amino alcohols.

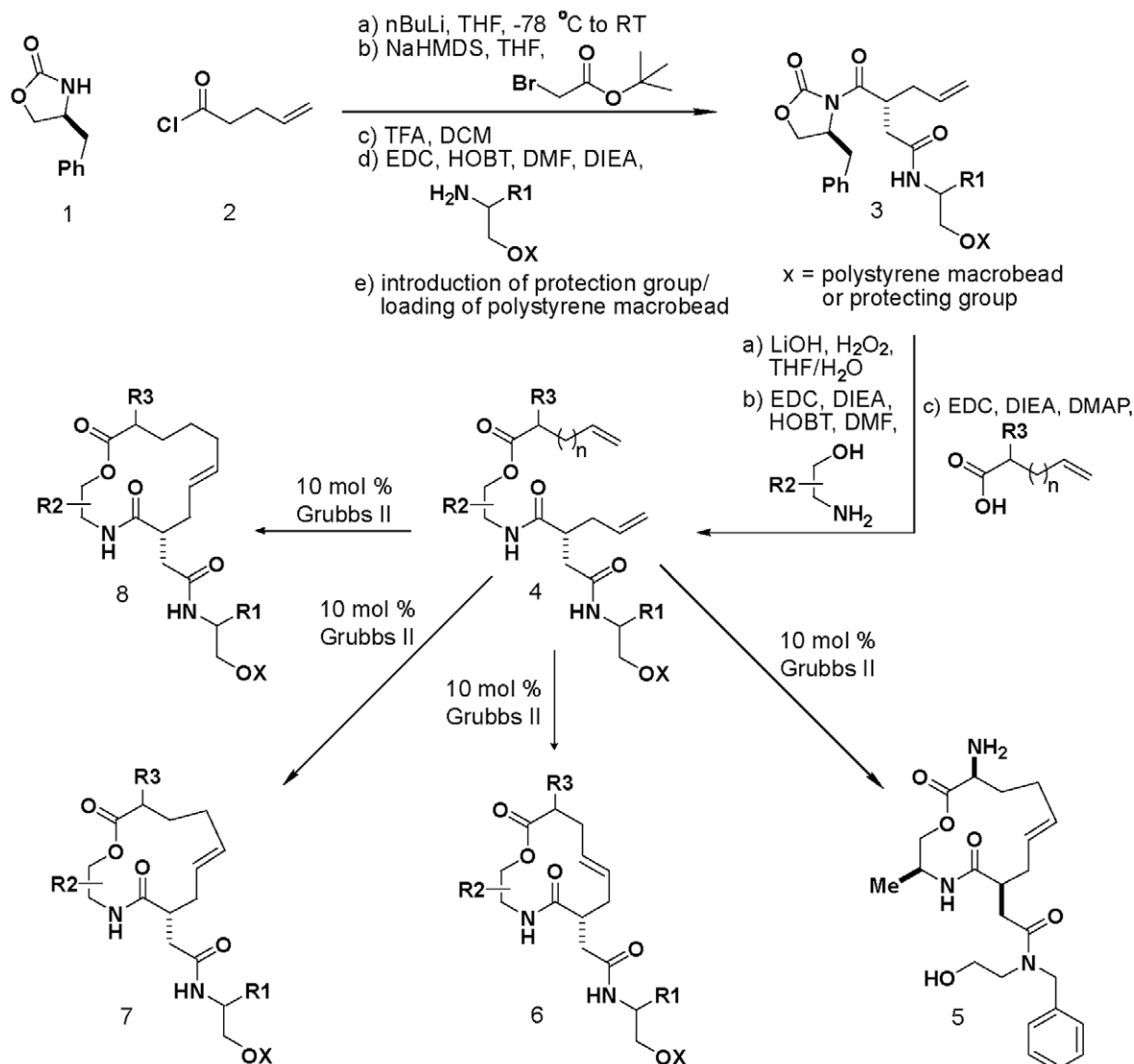
In the initial application of the synthetic pathway, we loaded the resulting alcohol onto polystyrene macrobeads.¹⁰ After cleaving the chiral auxiliary under standard conditions, the resulting acid was coupled with a variety of commercially available 1,2-aminoalcohols. Coupling reactions with acids of different chain lengths bearing terminal olefin groups yielded the acyclic macrolactone precursors. Ring-closing metathesis reactions (RCMs)¹¹ were used in the macrocyclization step. Using the (encoded) one macrobead/one stock solution approach,¹² 2070 compounds, including 12-, 13- and 14-membered macrocycles, were synthesized (S.L.S., unpublished results).

* Corresponding author. Tel.: +1 617 714 7438; fax: +1 617 714 8943.

E-mail address: lpeng@partners.org (L.F. Peng).

† These authors contributed equally.

‡ Senior Author.

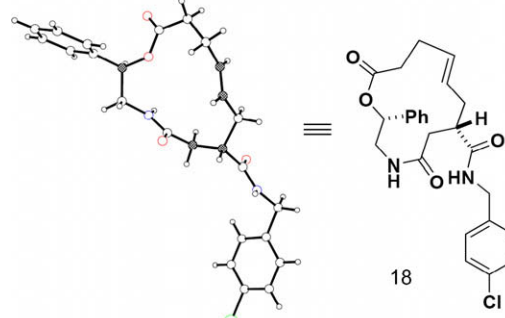


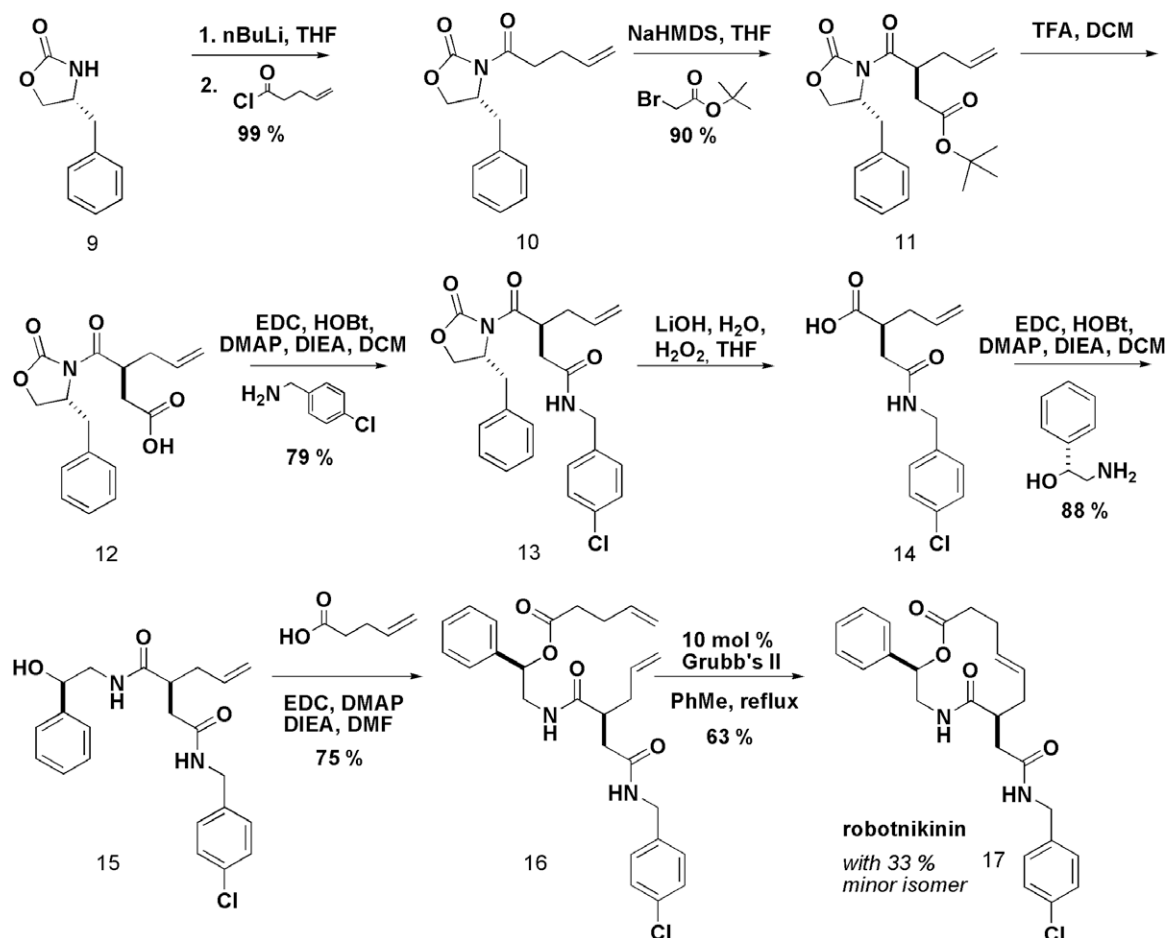
Scheme 1. A synthesis pathway yielding an array of macrocyclic compounds. Membered (12, 13 and 14) macrocycles can be generated starting from simple, commercially available building blocks. Note that both enantiomers of the chiral oxazolidinone⁹ were used to construct macrocycles with the R_1 building block in both stereochemical orientations in the solid and solution phase libraries. AML1 (**5**) was previously reported to bind purified ShhN based on small-molecule microarray (SMM) experiments verified with surface plasmon resonance (SPR).

The resulting compounds were arrayed onto microscope slides for small-molecule screening.¹³ The resulting small-molecule microarrays (SMMs)^{14–16} were screened for binding to purified Sonic Hedgehog N-terminal peptide (ShhN). Elsewhere, we have described the results of this screen that yielded **5**, which displayed concentration-dependent binding to ShhN by SPR with immobilized ShhN (Scheme 1).¹⁷ Encouraged by the ShhN-binding capacity of **5**, we adapted the chemistry described above to the solution-phase synthesis of a library of additional analogs (Scheme 2). The synthetic sequence was similar to a previously reported route,⁸ but differed with respect to the introduction of an asymmetric alkylation early in the sequence. After the removal of the oxazolidinone, subsequent amide and ester couplings afforded an acyclic precursor poised for RCM. The RCM reaction resulted in two isolated products, corresponding to the expected macrocycle

along with an unexpected acyl rearrangement isomer.⁸ In an earlier study¹⁷, we also reported the mechanistic evaluation of the most active compound from the library, named robotnikinin. Robotnikinin

⁸ The structure of the minor isomer in Scheme 2, resulting from acyl transfer, was characterized by X-ray crystallography (CCDC 748267).





Scheme 2. Robotnikinin was synthesized via the indicated pathway. The synthesis was carried out in solution phase with a 26% overall yield over eight linear steps.

binds the extracellular Sonic Hedgehog (Shh) protein and blocks Shh signaling in cell lines, human primary keratinocytes and a synthetic model of human skin. Shh pathway activity is rescued by small-molecule agonists of Smoothened, which functions immediately downstream of the Shh receptor, Patched. The structure of robotnikinin (17) and the synthetic pathway leading to it and its analogs is shown in Scheme 2.

Here, we describe the activity of the analogues in the Shh-LIGHT2 cell line (ATCC, Manassas VA),¹⁸ which is an NIH3T3 line with a stably incorporated Gli-luciferase construct along with zeocin and G418 resistance vectors to select for the transformed strains during normal culturing. Gli-dependent transcription is a robust metric for Shh pathway activity, and Shh pathway inhibitors have been shown to repress Gli activity in Shh-LIGHT2 cells.¹⁸ From the library, robotnikinin (17) showed strong concentration-dependent Gli repression, as measured with the Gli-luciferase construct of the Shh-LIGHT2 cells, a characteristic of Shh pathway inhibition.¹⁹ However, we hypothesized that if the interaction of robotnikinin was specific for ShhN, closely related analogues would have similar activity, while library members having differences in stereochemistry or ring size would have diminished abilities to suppress Gli activity.

As illustrated in Figure 1, 5 showed limited ability to inhibit Gli expression, with an EC_{max} reaching only 30% of the inhibitory capacity of cyclopamine. Modifications to the substituents of the macrocyclic core resulted in a marked increase in activity, with an EC₅₀ value 15 μ M and an EC_{max} reaching 93% of the inhibitory capacity of cyclopamine. Decreasing the size of the macrocycle from a 13-membered ring to a 12-membered ring leads to robot-

nikinin (17), the most active compound of the analogues. While the EC₅₀ value of robotnikinin was approximately 4 μ M, both compounds retained similar abilities for maximum repression of Gli activity (Fig. 1, Table 1).

Strikingly, by inserting a single methylene unit into the scaffold of robotnikinin and reversing the orientation of the two stereogenic centers, Gli suppression was ablated (compound 19, Figs. 1 and 2). Furthermore, neither compound displayed differences in cytotoxicity at any concentration (see Supplementary data) as measured by Cell Titer Glo (Promega, Madison, WI).

These findings motivated us to test stereochemically and skeletally related compounds in the Shh-LIGHT2 Gli reporter assay. The stereochemical inverse of robotnikinin (2S,6R) had reduced activity with an EC_{max} reaching only 60% of the inhibitory capacity of cyclopamine, and an EC₅₀ of approximately 15 μ M (Table 1). The corresponding 14-membered compound (2S,6R) had no detectable activity in the Shh-LIGHT2 cell line at concentrations ranging from 3.9 μ M to 125 μ M. The 14-membered analogue of robotnikinin (2R,6S) had no detectable Gli repression.

We also investigated the effect of more subtle stereochemical alterations in the robotnikinin scaffold in the context of Gli repression in the Shh-LIGHT2 line. When the stereochemistry was altered to the (2R,6R) configuration with the identical 12-membered ring size, the percent cyclopamine EC_{max} dropped to 68% from 91% with a similar EC₅₀ value. Adding another methylene unit to the macrolactone scaffold (2R,6R) did not change the activity appreciably, but the 14-membered macrolactone analogue (2R,6R) had significantly decreased potency, with an EC_{max} only 37% of that of cyclopamine, and did not show a change in response with a change in dose. The

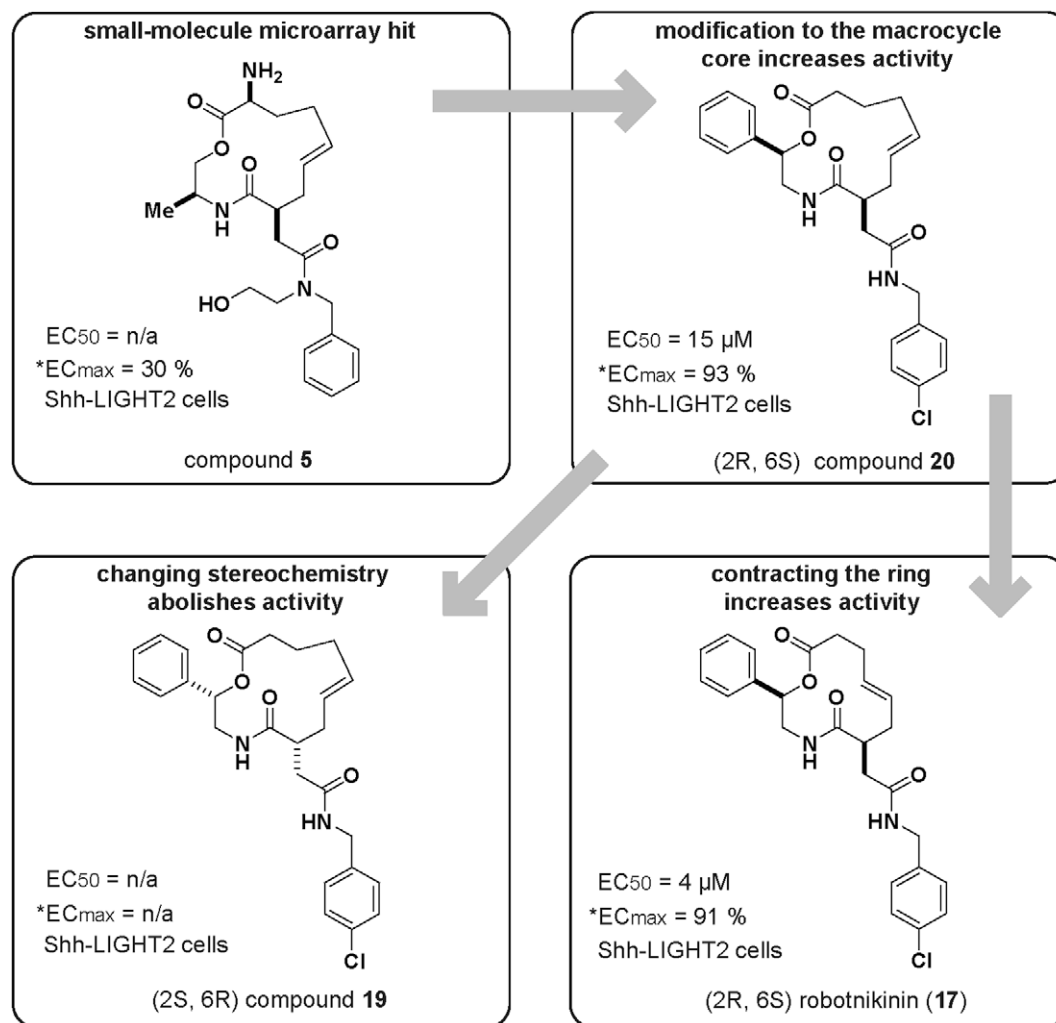


Figure 1. Investigating trends in activity. Appendage modifications, modifications to the stereochemistry, and ring size dramatically influence the activity in the Shh-LIGHT2 cell line. [*] EC_{max} denotes the percent activity of maximum inhibition rendered by cyclopamine.

Table 1
Shh-LIGHT2 activity of robotnikinin analogues

(n, 2, 6)	Gli EC ₅₀ ^a	Gli EC _{max}	% EC _{max} ^b	K _D ^c	Cytotoxicity ^d
(0, n/a, R)	15 μM	125 μM	50% ^e	>50	None
(1, n/a, R)	31 μM	125 μM	66%	10.0	None
(2, n/a, R)	30 μM	125 μM	53%	38.2	None
(0, n/a, S)	60 μM	125 μM	55% ^e	23.8	None
(1, n/a, S)	70 μM	125 μM	74%	>50	None
(2, n/a, S)	60 μM	125 μM	70% ^e	5.7	None
(0, S,R)	15 μM	125 μM	60% ^e	8.7	None
(1, S,R) (19)	n/a	n/a	n/a	3.1	None
(2, S,R)	n/a	n/a	n/a ^d	4.5	None
(0, S,S)	10 μM	15.6 μM	57% ^e	0.57	>15.6 μM
(1, S,S)	20 μM	125 μM	71% ^e	>50	None
(2, S,S)	n/a	n/a	n/a	n/a	>31 μM
(0, R,S) (17)	4 μM	62.5 μM	91% ^e	3.1	None
(1, R,S) (20)	15 μM	125 μM	93% ^e	1.8	None
(2, R,S)	n/a	n/a	n/a	n/a	None
(0, R,R)	7 μM	62.5 μM	68%	>50	None
(1, R,R)	4 μM	15.6 μM	71%	8.9	None
(2, R,R)	n/a	125 μM	37%	n/a	None

Robotnikinin analogues were synthesized in solution phase and tested in the Shh-LIGHT2 cell line. n = 0, 1, 2 designates 12, 13 and 14-membered macrocycles, respectively. The stereochemical designation of n/a designates the absence of a substituent at that position. See Figures 1 and 2 for full structural information.

^a Gli activity was determined with *Bright Glo* luciferase assay system (Promega: Madison, WI). Values represent approximations based on concentration curves (see Supplementary data).

^b % EC_{max} denotes the percentage of inhibitory effect relative to the EC_{max} of cyclopamine.

^c SPR binding data to ShhN are represented in μM concentrations.

^d Cytotoxicity measurements were made with *Cell Titer Glo* (Promega: Madison, WI).

^e These data are taken relative to mock treatment, which has resulted in luciferase reporter values comparable to 6 μM cyclopamine. For cytotoxic compounds, % EC_{max} was calculated with respect to the highest effective non-cytotoxic concentration.

robotnikinin diastereomer (2*S*,6*S*) displayed cytotoxicity at concentrations above 16 μ M in Shh-LIGHT2 cells and only modest inhibitory activity at the highest non-cytotoxic concentration. The related 13-membered macrolactone (2*S*,6*S*) resulted in a five-fold decrease in the EC_{50} , from 4 μ M to 20 μ M, but only a modest 20% drop in the % cyclopamine EC_{max} relative to robotnikinin. The 14-membered analogue (2*S*,6*S*) was found to be cytotoxic above 31 μ M, and had poor solubility in SPR studies. The related compounds without substituents at the 2-position featured relatively decreased potency, although at extremely high concentrations several of these compounds displayed EC_{max} levels at approximately 70% of cyclopamine's EC_{max} (Table 1).

Many of the compounds like **1**, and robotnikinin, bound purified ShhN in a stoichiometric manner, as verified by surface plasmon resonance (SPR) experiments. Furthermore, the apparent off-rate of robotnikinin was significantly longer than that of its (2*S*,6*R*) 13-membered homolog (see Fig. 3). This may help explain why both compounds bind to ShhN, but one lacks significant activity. For the remainder of the inactive compounds tested by SPR, 13-membered (2*S*,6*R*), 14-membered (2*S*,6*R*), and 14-membered (2*R*,6*R*), we observed was no measurable affinity for ShhN. For the remainder of the compounds that were found to be active in the Shh-LIGHT2 cell line, we observed dose-dependent affinity for the ShhN as measured by SPR. This presents the possibility

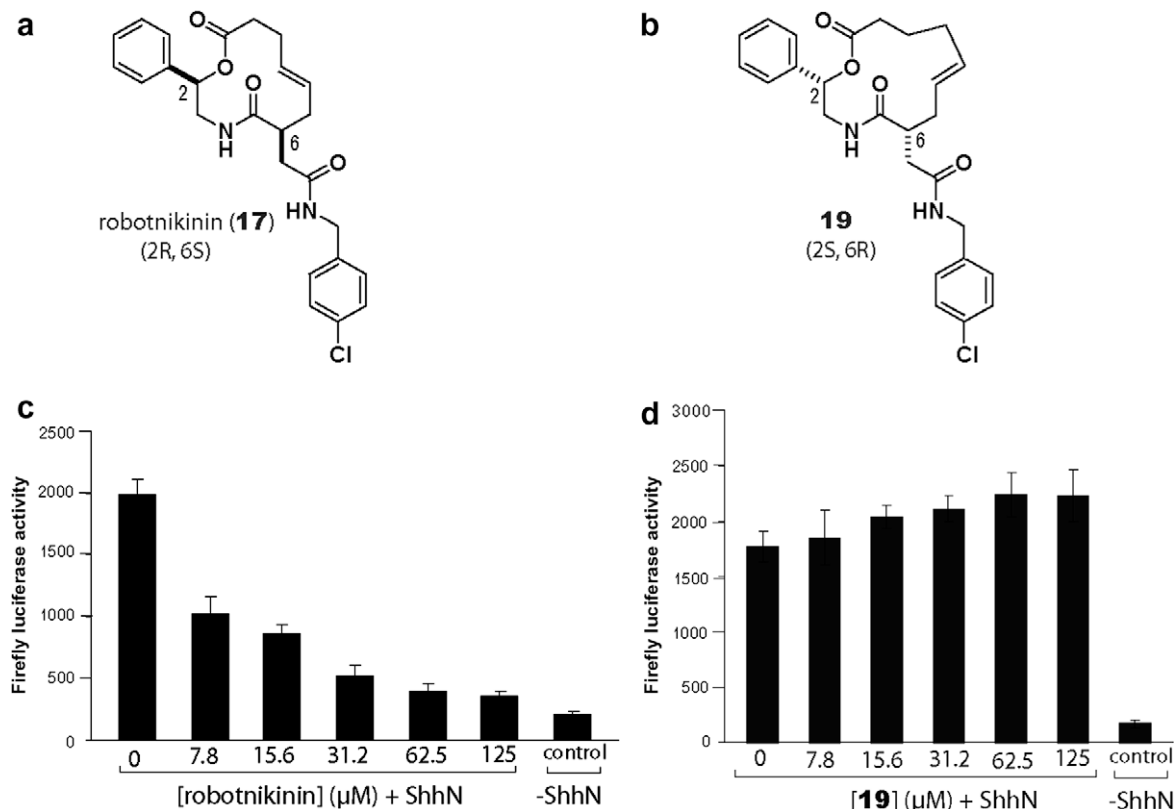


Figure 2. (a) Structure of robotnikinin; (b) structure of a robotnikinin analogue with an extra methylene unit inserted in the macrocycle and stereogenic centers in the opposite configuration of robotnikinin; (c and d) dose curves of robotnikinin and a robotnikinin analogue, respectively, in an Shh-LIGHT2 cell line. ShhN represents ShhN-conditioned DMEM with 0.5% (v/v) calf serum.

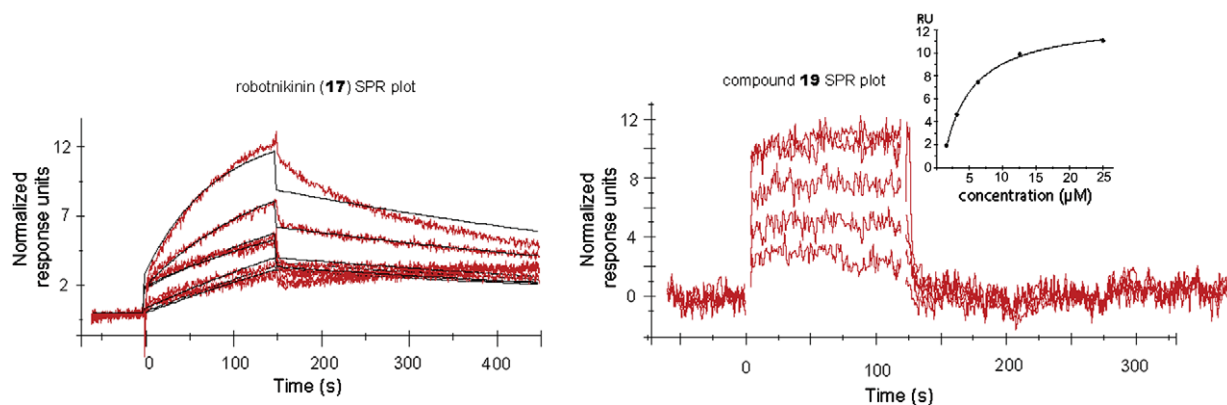


Figure 3. SPR curves. Robotnikinin (left) and its ($n=1$, 2*S*,6*R*) isomer (right) are shown. All data are background subtracted from DMSO. The difference in off-rates is significant. The curves were generated from SPR experiments in PBS buffer with 5% (v/v) DMSO.

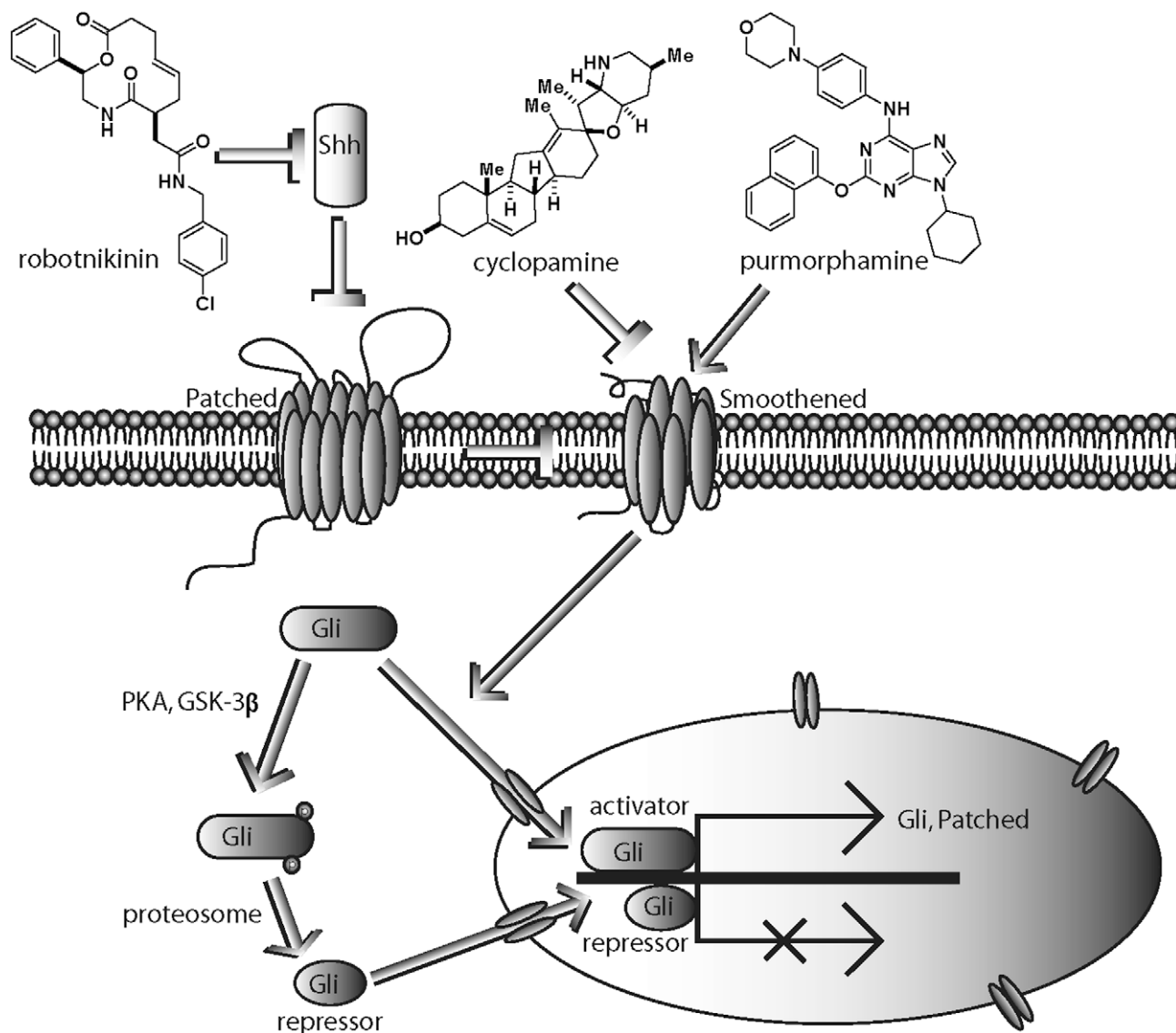


Figure 4. The Shh pathway initiates with the Shh ligand binding to its receptor Patched1 (Ptc1), which de-represses smoothened (Smo) and allows the active form of Gli2 to enter the nucleus and activate target genes which include *Gli1* and *Ptc1*. We have demonstrated that inhibition of the Shh pathway can result from the binding of a small molecule to Shh.

that, like robotnikinin, other compounds in this class inhibit Gli activity by interfering with the ability of ShhN to interact effectively with its receptor. Differences in ring size and stereochemistry leading to alterations in the nature and conceivably location of the binding, may account for differences in the degree of biological activity.

We hypothesize that the active compounds may perturb binding interactions between Shh and its associated proteins so it cannot interact effectively with the Ptc1 receptor (Fig. 4).²⁰ In a previous report, we established the use of the *Ptc1*^{-/-} cell line,²¹ as well as co-administration with Smoothened agonists purmorphamine and SAG in various Shh-responsive cells for robotnikinin.¹⁷ Studies in a constitutively active mouse embryonic fibroblast (MEF) *Ptc1*^{-/-} cell line where both *Ptc1* alleles are replaced with a β -galactosidase reporter under control of Gli transcription, indicated that the compounds listed in Table 1 are not effective at Gli repression without the intact Ptc1 receptor (B.Z.S., L.F.P. and S.L.S., unpublished results). Taken together, the data suggest that the compounds shown here to be active in the context of Shh pathway inhibition may likely exert their effects at the Shh level. Fur-

ther mechanistic experiments to explore this possibility will be investigated in future efforts.

Acknowledgements

We thank Dr. Douglas M. Ho and Dr. Shao-Liang Zheng of the Center for Crystallographic Studies at Harvard University for the X-ray crystallographic analysis. We thank James K. Chen, Kazuo Nakai, Andrew M. Stern, Gregory T. Copeland, Damian W. Young, and Timothy A. Lewis for their helpful suggestions. L.F.P. is supported by grants from the National Pancreas Foundation, the American Gastroenterological Association, and the American Liver Foundation. This research was supported by the National Institute of General Medical Sciences (GM-38627, awarded to S.L.S.) S.L.S. is an investigator with the Howard Hughes Medical Institute.

Supplementary data

Supplementary data associated with this article can be found, in the online version, at [doi:10.1016/j.bmcl.2009.09.089](https://doi.org/10.1016/j.bmcl.2009.09.089).

References and notes

1. Kittendorf, J. D.; Beck, B. J.; Buchholz, T. J.; Seufert, W.; Sherman, D. H. *Chem. Biol.* **2007**, *14*, 944.
2. Gokhale, R. S.; Hunziker, D.; Cane, D. E.; Khosla, C. *Chem. Biol.* **1999**, *6*, 117.
3. Bluhm, M. E.; Kim, S. S.; Dertz, E. A.; Raymond, K. N. *J. Am. Chem. Soc.* **2002**, *124*, 2436.
4. Feyen, F.; Cachoux, F.; Gertsch, J.; Wartmann, M.; Altmann, K. H. *Acc. Chem. Res.* **2008**, *41*, 21.
5. Harding, M. W.; Galat, A.; Uehling, D. E.; Schreiber, S. L. *Nature* **1989**, *341*, 758.
6. Nakatsuka, M.; Ragan, J. A.; Sammakia, T.; Smith, D. B.; Uehling, D. E.; Schreiber, S. L. *J. Am. Chem. Soc.* **1990**, *112*, 5583.
7. Rosen, M. K.; Standaert, R. F.; Galat, A.; Nakatsuka, M.; Schreiber, S. L. *Science* **1990**, *248*, 863.
8. Lee, D.; Sello, J.; Schreiber, S. L. *J. Am. Chem. Soc.* **1999**, *121*, 10648.
9. Evans, D. A.; Ellman, J. A. *J. Am. Chem. Soc.* **1989**, *111*, 1063.
10. Blackwell, H. E.; Pérez, L.; Stavenger, R. A.; Tallarico, J. A.; Eatough, E. C.; Folley, M. A.; Schreiber, S. L. *Chem. Biol.* **2001**, *8*, 1167.
11. Grubbs, R. H.; Chang, S. *Tetrahedron* **1998**, *54*, 4413.
12. Clemons, P. A.; Koehler, A. K.; Wagner, B. K.; Spriggs, T. G.; Spring, D. R.; King, R. W.; Schreiber, S. L.; Foley, M. A. *Chem. Biol.* **2001**, *8*, 1183.
13. Bradner, J. E.; McPherson, O. M.; Mazitschek, R.; Barnes-Seeman, D.; Shen, J. P.; Dhaliwal, J.; Stevenson, K. E.; Duffner, J. L.; Park, S. B.; Neuberg, D. S.; Nghiem, P.; Schreiber, S. L.; Koehler, A. K. *Chem. Biol.* **2006**, *13*, 493.
14. Macbeath, G.; Koehler, A. N.; Schreiber, S. L. *J. Am. Chem. Soc.* **1999**, *121*, 7967.
15. Barnes-Seeman, D.; Park, S. B.; Koehler, A. N.; Schreiber, S. L. *Angew. Chem., Int. Ed.* **2003**, *42*, 2376.
16. Koehler, A. N.; Shamji, A. F.; Schreiber, S. L. *J. Am. Chem. Soc.* **2003**, *125*, 8420.
17. Stanton, B. Z.; Peng, L. F.; Maloof, N.; Nakai, K.; Wang, X.; Duffner, J. L.; Taveras, K. M.; Hyman, J. M.; Lee, S. W.; Koehler, A. N.; Chen, J. K.; Fox, J. L.; Mandinova, A.; Schreiber, S. L. *Nat. Chem. Biol.* **2009**, *5*, 154.
18. Taipale, J.; Chen, J. K.; Cooper, M. K.; Wang, B.; Mann, R. K.; Milenkovic, L.; Scott, M. P.; Beachy, P. A. *Nature* **2000**, *406*, 1005.
19. Chen, J. K.; Taipale, J.; Young, K. E.; Maiti, T.; Beachy, P. A. *PNAS* **2002**, *99*, 14071.
20. Tenzen, T.; Allen, B. L.; Cole, F.; Kang, J. S.; Krauss, R. S.; McMahon, A. P. *Dev. Cell* **2006**, *10*, 647.
21. Sinha, S.; Chen, J. K. *Nat. Chem. Biol.* **2006**, *2*, 29.